Anisotropic minimal conductivity of graphene bilayers

Ali G. Moghaddam and Malek Zareyan
Institute for Advanced Studies in Basic Sciences, P.O. Box 45195-1159, Zanjan 45195, Iran
(Received 8 August 2008; revised manuscript received 15 December 2008; published 5 February 2009)

The Fermi line of bilayer graphene at zero energy is transformed into four separated points positioned trigonally at the corner of the hexagonal first Brillouin zone. We show that as a result of this trigonal splitting the minimal conductivity of an undoped bilayer graphene strip becomes anisotropic with respect to the orientation θ of the connected electrodes and finds a dependence on its length L on the characteristic scale $\ell=\pi/\Delta k\simeq 50$ nm determined by the inverse of k-space distance of two Dirac points. The minimum conductivity increases from a universal isotropic value $\sigma_{\perp}^{\min}=(8/\pi)e^2/h$ for a short strip $L\ll\ell$ to a higher anisotropic value for longer strips, which in the limit of $L\gg\ell$ varies from $(7/3)\sigma_{\perp}^{\min}$ at $\theta=0$ to $3\sigma_{\perp}^{\min}$ over an angle range $\Delta\theta\sim\ell/L$.

DOI: 10.1103/PhysRevB.79.073401 PACS number(s): 73.23.Ad, 73.63.−b, 81.05.Uw

The recent realization of isolated graphene,[1–3] a two-dimensional (2D) hexagonal lattice of carbon atoms, and its bilayer[4] has been followed by intensive studies which explored many intriguing properties of these new carbon-based materials.[5] They are zero-gap semiconductors with their valance and conduction bands touching each other at the corners of the hexagonal first Brillouin zone known as Dirac points. This specific band structure in connection with the pseudospin aspect which characterizes the relative amplitude of the electron wave function on two different sublattices of the hexagonal structure has given the carriers a pseudorelativistic chiral nature.[2,4] The chirality is believed to be the origin of most of the peculiarities of quantum transport effects in single and bilayer graphenes.[5–7]

One of the most important observations in graphene systems is the existence of a nonzero minimal conductivity in the limit of vanishing carrier density (at Dirac points).[2] This effect which had been predicted theoretically long before the experimental synthesis of graphene[8] has been the subject of several recent theoretical investigations, and in most studies a universal value $\sigma_0^{\min}=(4/\pi)e^2/h$ for minimum conductivity of monolayer graphene was found.[9–14] Although the theoretical value is π times smaller than the value measured in the early experiments, more recent experiments have confirmed the predicted universal value $\sigma_0^{\min}$ for wide and short graphene strips.[15,16]

For bilayer graphene the minimum conductivity is also measured to be on the order of e^2/h.[4,17] Despite the similarity of the chiral nature in single and bilayer graphenes, the low-energy spectrum in the bilayer is drastically different from the linear dispersion of massless Dirac fermions in the monolayer. The spectrum in bilayer, which has a parabolic form at high energies, acquires strong trigonal warping at low energies and undergoes the so-called Lifshitz transition at which the Fermi line is broken into four separated pockets.[18] In the limit of zero Fermi energy the pockets shrink into the points of which one is located at the Dirac point and three others positioned around it in a trigonal form [see Fig. 1(a)]. The aim of the present Brief Report is to study the effect of this Dirac point trigonal splitting on the minimum conductivity of the bilayer, which will also allow us to distinguish between the effects of masslessness and chirality. We employ the realistic model of a wide undoped bilayer strip of length L as the scattering region connecting two highly doped regions as electrodes. Using a full Hamiltonian which takes into account all intralayer and interlayer hoppings between nearest-neighbor atomic sites, we find that the effect of the trigonal splitting in the minimum conductivity depends on L as compared to a characteristic length $\ell=\pi/\Delta k\simeq 50$ nm determined by the inverse of the k-space separation Δk of two split Dirac points.

For a short strip of $L\ll\ell$ the effect of trigonal splitting is negligible and $\sigma_{\perp}^{\min}=(8/\pi)e^2/h$, which is twice the minimum conductivity of a monolayer showing that in this limit the bilayer behaves as two independent single layers connected in parallel. For a finite length strip the minimal conductivity increases above $\sigma_{\perp}^{\min}$ and finds a dependence on the angle θ between the orientation of the electrodes and the hexagonal lattice symmetry axis. We find that for a long strip $L\gg\ell$ the anisotropic minimum conductivity $\sigma^{\min}(\theta)$ increases from $(7/3)\sigma_{\perp}^{\min}$ at $\theta=0$ to $3\sigma_{\perp}^{\min}$ over an angle range $\Delta\theta\sim\ell/L$. Our results reveal the importance of trigonal splitting of the zero-energy spectrum on the minimal conductivity of bilayer graphene.

To this end, there have been few theoretical investigations devoted to the minimal conductivity in bilayer graphene.[19–24] In Ref. 21 a wide bilayer sheet with a constant perpendicular interlayer hopping is considered to connect two heavily doped electrode regions. This model, which ignores the trigonal splitting, results in a minimum conductivity $\sigma^{\min}=\sigma_{\perp}^{\min}$,[20,21] establishing the fact that for high-energy electrons injected from the metallic electrodes, the constant interlayer hopping does not cause any significant effect and the bilayer sheets behave as two monolayers in parallel. On the other hand, authors of Refs. 22 and 23 have taken into account the effect of strong trigonal warping within, respectively, the Born approximation and Kubo formula. They have found an isotropic and constant minimal conductivity $(24/\pi)e^2/h$, which is three times larger than $\sigma_{\perp}^{\min}$ obtained in Refs. 20 and 21. However, we note that the models employed in Refs. 22 and 23 do not include the effect of electrodes which are present in a realistic experimental setup for conductivity measurement. This could be in particular important in graphene contacts due to the chirality of the carriers and the

 ©2009 The American Physical Society

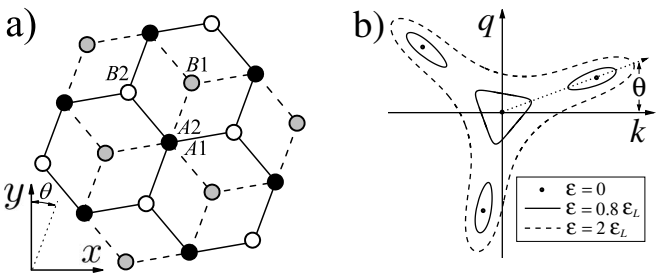

FIG. 1. (a) The bilayer lattice structure projected onto the x-y plane. Bonds between $A1$-$B1$ ($A2$-$B2$) in bottom (top) layer are indicated by dashed (solid) lines; θ is the angle between the lattice symmetry axis and the y axis. (b) Constant-energy lines around the corner of the hexagonal first Brillouin zone for different energies (measured in units of Lifshitz transition energy $\varepsilon_L \approx 1$ meV) near the neutrality point.

resulting Klein tunneling phenomena.[6,7] Our study, taking into account both the trigonal splitting and the electrode effect, reveals anisotropy of the minimal conductivity and its dependence on L/ℓ which also clarifies the origin of the disagreement between the two above predictions.

We consider a ballistic bilayer graphene sheet in x-y plane consisting of an undoped strip of length L and width W and two heavily doped regions for $x<0$ and $x>L$ on top of which bias electrodes are deposited. The interfaces between electrode regions and bilayer strip are oriented parallel to y axis making an angle θ with respect to the symmetry axis of the bilayer lattice as indicated in Fig. 1(a).

Bilayer graphene is made of two coupled single-layer graphene with different sites $A1, B1$ in the bottom layer and $A2, B2$ in the top layer. The two layers are arranged according to Bernal stacking in which every $A1$ site of the bottom layer lies directly below an $A2$ site in the top layer, as shown in Fig. 1(a). Within the tight-binding model of graphite[5,24] we consider all the nearest-neighbor hoppings. The intralayer hoppings between the sites $A1$-$B1$ and $A2$-$B2$ are parametrized by the single energy $t \approx 3$ eV. There are two types of interlayer hoppings: $A1$-$A2$ and $B1$-$B2$ which are characterized by the energies $t_\perp \approx 0.4$ eV and $t_3 \approx 0.3$ eV, respectively. The other possible hoppings including γ_4 between $A1$-$B2$ and $A2$-$B1$ have much smaller values and are not considered.[24] In addition since the main effect of γ_4 is to break electron-hole symmetry, it cannot affect minimal conductivity significantly.[25] The given values for the hopping energies are well-known typical values for graphite; however, they are mostly used in the graphene literature.[24,25] For bilayer graphene itself some experiments have reported different values for $t_3 \approx 0.1-0.2$ eV,[26] which is still on the order of 0.1 eV and will not change our main results.

The resulting tight-binding Hamiltonian is written in k space. The hexagonal first Brillouin zone of bilayer graphene contains six corners. Among them two are inequivalent specifying the valleys K and K'. In the absence of intervalley scattering,[5] the valleys are degenerate and it is sufficient to consider only one valley. Low-energy excitations with 2D wave vector $\mathbf{k} \equiv (k,q)$ around one of these valleys, say valley K, is governed by the Hamiltonian of the form[18]

$$\mathcal{H}(\mathbf{k}) = \begin{pmatrix} 0 & \hbar v k_- & t_\perp & 0 \\ \hbar v k_+ & 0 & 0 & \hbar v_3 k_- \\ t_\perp & 0 & 0 & \hbar v k_+ \\ 0 & \hbar v_3 k_+ & \hbar v k_- & 0 \end{pmatrix}, \quad (1)$$

which operates in the space of four-component spinors of the form $\Psi = e^{ikx+iqy}(\psi_{A1}, \psi_{B1}, \psi_{A2}, \psi_{B2})$, where each component determines the wave-function amplitude at the corresponding site of the bilayer unit cell. The characteristic velocities $v = 3ta/2\hbar$ and $v_3 = 3t_3 a/2\hbar$ (a is the lattice constant) are associated with the hopping energies t and t_3, respectively. We note that the complex wave vectors $k_\pm = e^{\mp i\theta}(k \pm iq)$ depend on the misorientation angle θ.

The quasiparticle spectrum $\varepsilon(k,q)$ is obtained from the eigenvalue equation of Hamiltonian (1), which reads

$$(\varepsilon^2 - |\hbar v \mathbf{k}|^2)^2 - \varepsilon^2(t_\perp^2 + |\hbar v_3 \mathbf{k}|^2) + |\hbar v_3 \mathbf{k}|^2 t_\perp^2 = (\hbar v)^2 t_\perp \hbar v_3 [e^{3i\theta}(k - iq)^3 + e^{-3i\theta}(k + iq)^3]. \quad (2)$$

It is clear that the right-hand side of this equation produces trigonal warping of constant-energy lines, with a strength given by the ratio $\delta = v_3/v$. Figure 1(b) shows constant-energy lines for three energies $\varepsilon/\varepsilon_L = 0$, 0.8, and 2, where $\varepsilon_L = t_\perp \delta^2/4$ is the characteristic energy at which the Lifshitz transition takes place. While at $\varepsilon = 2\varepsilon_L$ the energy line, despite its strong trigonal warping, is a continuous line, at $\varepsilon = 0.8\varepsilon_L$ it breaks into four pockets whose enclosed area decreases with lowering energy and finally at $\varepsilon = 0$ shrinks into the four points. The central point is located at $|\mathbf{k}| = 0$ and the other three leg points at a constant distance $|\mathbf{k}| = \Delta k = t_\perp v_3/\hbar v^2$ from the center and in the directions determined by angles $\theta_n = \arctan(q_n/k_n) = \theta + 2(n-1)\pi/3$, where $n = 1$, 2, and 3 [see Fig. 1(b)].

Dirac point splitting will have two main effects on the transport of carriers through the bilayer strip. First it introduces a length scale $\ell = \pi/\Delta k = \pi\hbar v/t_\perp \delta \approx 50$ nm as the effective range of the scattering potential which could mix the states at the four Dirac points. This length scale is 1 order of magnitude larger than interlayer coupling length $l_\perp = \hbar v/t_\perp$ introduced in Ref. 21. For realistic graphene samples of a few 100 nm length, $L > \ell$ and the variations over this length scale should be taken into account. The potential profile varies over the length L of the strip. For $L \lesssim \ell$ the scattering potential is short enough to cause strong inter-Dirac point scattering and consequently the scattering states at these points are mixed. On the other hand, for $L \gg \ell$ the states of the Dirac points are well separated and do not mix. Second, it causes anisotropy of the scattering states due to the orientation of the leg points. As we will explain in the following, these effects result in a length-dependent anisotropic minimal conductivity for the bilayer strip.

Within the scattering formalism we find the transmission amplitude of electrons through the bilayer strip. An electronic state is specified by the energy ε and the transverse wave vector q, which are conserved in the scattering process. We find the eigenstates of Hamiltonian (1) in three regions of left ($x<0$) and right ($x>L$) electrodes and the bilayer strip ($0<x<L$). In general for a given ε and q there are four values of longitudinal momentum k [solutions of Eq. (2)]

with four corresponding eigenstates in each region.

Inside the strip at the neutrality point $\varepsilon=0$, the four solutions $(k_i, i=1,\ldots,4)$ of Eq. (2) have the form

$$k_{1,2} = k_{3,4}^{*} = iq + (\pi/2\ell)\exp(-3i\theta)(1 \pm \sqrt{1+8iq\ell\,\exp(3i\theta)/\pi}).$$

The corresponding eigenstates are given by

$$\phi_{1,2} = e^{ik_{1,2}x+iqy}\left(0, -\frac{e^{-i\theta}}{l_\perp}, k_{1,2}-iq, 0\right), \tag{3}$$

$$\phi_{3,4} = e^{ik_{3,4}x+iqy}\left(k_{3,4}+iq, 0, 0, -\frac{e^{i\theta}}{l_\perp}\right). \tag{4}$$

In general for a given q all four states inside the strip are evanescent having complex k_i $(i=1,\ldots,4)$ with exceptions of the Dirac points with $q_0=0$ and $q_n=(\pi/\ell)\sin(\theta_n)$ $(n=1,2,3)$ at which two of the k_i's are real representing propagating states in the strip.

Inside the highly doped electrode regions a very large potential $-U_0$ is applied. We assume that for all states contributing in transport $\hbar v q \ll U_0$ provided that U_0 is much larger than all other energy scales in Hamiltonian (1). By this assumption the longitudinal momenta of all states inside electrode regions have a constant magnitude $k_0=U_0/\hbar v \gg q$. Inside each electrode for certain q there are two right-going eigenstates $\phi_\pm^R=\exp(ik_0x+iqy)[1,\exp(-i\theta),\pm 1,\pm\exp(i\theta)]$ and two left-going eigenstates $\phi_\pm^L=\exp(-ik_0x+iqy)$ $[1,-\exp(-i\theta),\pm 1,\mp\exp(i\theta)]$.

For two left-going incident states from the left electrode $(x<0)$ the scattering states in three different regions have the form

$$\Psi_\pm = \begin{cases} \phi_\pm^R + r_+^\pm \phi_+^L + r_-^\pm \phi_-^L, & x<0, \\ \sum_{i=1}^{4} c_i^\pm \phi_i, & 0<x<L, \\ t_+^\pm \phi_+^R + t_-^\pm \phi_-^R, & x>L, \end{cases} \tag{5}$$

where the coefficients $c_i^\pm$ and reflection and transmission amplitudes $r_\pm^\pm$ and $t_\pm^\pm$ have to be determined by imposing the continuity condition of the wave functions at the boundaries $x=0,L$.

We calculate the conductance at zero temperature from the Landauer-Buttiker formula,

$$\frac{G}{G_0} = \frac{W}{2\pi}\int_{-\infty}^{\infty} T(q)dq, \tag{6}$$

where $T(q)=|t_+^+|^2+|t_+^-|^2+|t_-^+|^2+|t_-^-|^2$ is the sum of transmission probabilities of the two states $\Psi_\pm$ and $G_0=4e^2/h$ is 4 times the conductance quantum to take into account the valley and spin degeneracies. The conductivity of the bilayer strip is obtained by the relation $\sigma=(L/W)G$.

We have obtained $T(q)$ as a function of the length L and the orientation angle θ. For a short strip with $L \ll \ell$ the transmission probability takes the form

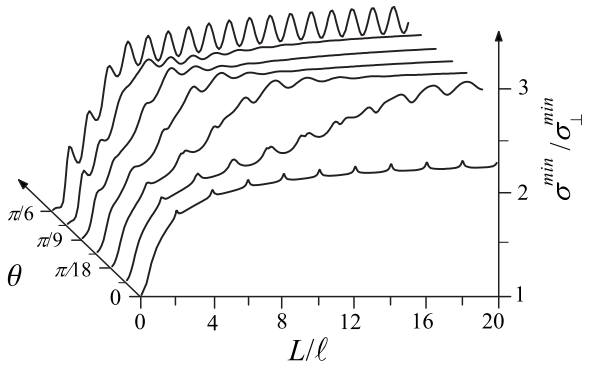

FIG. 2. Minimal conductivity in units of $\sigma_\perp^{\min}=(8/\pi)(e^2/h)$ of a wide strip of undoped bilayer graphene versus its length L for different orientations θ of the hexagonal lattice symmetry axis with respect to the electrodes. L is measured in units of $\ell=\pi/\Delta k$ with Δk being the k-space distance of two trigonally split Dirac points.

$$T(q) = \frac{1}{\cosh^2[(q-q_c)L]} + \frac{1}{\cosh^2[(q+q_c)L]}, \tag{7}$$

which shows two maxima at the point $q=\pm q_c = \pm\,\mathrm{arcsinh}(L/2l_\perp)/L$. Around these points $T(q)$ decays exponentially within a scale of the order $\Delta q \sim 1/L$ which is for a short strip much larger than $\Delta k=\pi/\ell$. Thus $T(q)$ is almost constant within the scale Δk which implies that the Dirac point splitting and the associated anisotropy of the spectrum are not revealed in the transmission of the carriers. This is the result of strong mixing of the states around the four Dirac points via scattering through the bilayer strip. The resulting isotropic minimum conductivity $\sigma_\perp^{\min}=2\sigma_0^{\min}$ which is twice of the minimum conductivity for a single layer.

For a finite L/ℓ the minimum conductivity increases above $\sigma_\perp^{\min}$. This is shown in Fig. 2 where we have plotted $\sigma^{\min}$ as a function of L/ℓ for different orientations θ. For $L/\ell \gtrsim 1$ the increased minimum conductivity finds a θ dependence as the result of trigonal splitting of the Dirac point. In this case the anisotropy of $\sigma^{\min}$ is spread over the range $0<\theta<\pi/6$. We note that the increase in $\sigma^{\min}$ is associated with an oscillatory variation due to quantum interference effects in the bilayer strip. Increasing L/ℓ further to approach the limit of a long strip $L \gg \ell$ the range of anisotropy becomes narrower. In this limit and for the angles not too close to $\theta=0,\pi/6$ we obtain the following relation for the transmission probability:

$$T(q) = \sum_{n=0,3} \frac{1}{\cosh^2\{\alpha_n(\theta)[q-q_n(\theta)]L\}}, \tag{8}$$

where the summation is taken over four transverse coordinates of the Dirac points, q_n, with $\alpha_0=1$ and $\alpha_n(\theta)=3/[5-4\cos(2\theta_n)]$ for $n=1,2,3$. This result shows that the transmission probability consists of four resonant peaks at the points q_n, whose width is on the order of $\Delta q \sim 1/L \ll \Delta k$. The effect of the Dirac point splitting is, thus, revealed in the transmission process. For θ approaching 0 and $\pi/6$ the transverse coordinates of the two resonant peaks $q_0 \to q_1$ and $q_1 \to q_2$, respectively, and the corresponding peaks overlap. For these cases Eq. (8) is not applicable since we have con-

sidered four Dirac points contributed independently in this equation. In the case of $\theta=0$ from Eqs. (5) and (6) we find that the contribution of the conductivity from the peaks at $q_0=q_1=0$ is on the order of $\delta^2 e^2/h$ which is negligibly small. So there are only contributions from the points q_2 and q_3 which result in a minimum conductivity $\sigma^{\min}_{\theta=0}=(7/3)\sigma^{\min}_{\perp}$. In contrast to the $\theta=0$ case, for $\theta=\pi/6$ the overlapped resonant peaks make the same contributions as two independent peaks. Thus, for all orientations $0\lesssim\theta<\pi/6$, except the angles $\theta\lesssim\ell/L$, we can use Eq. (8) for $T(q)$ which leads to the constant minimal conductivity $\sigma^{\min}=3\sigma^{\min}_{\perp}$ (see Fig. 2). This means that $\sigma^{\min}$ is anisotropic over the vanishingly small range $\Delta\theta\sim\ell/L$ with an amplitude $\Delta\sigma^{\min}=(2/3)\sigma^{\min}_{\perp}$. For $L\gg\ell$ the conductivity has isotropic value $\sigma^{\min}=3\sigma^{\min}_{\perp}$, as is expected from the D_{6h} lattice symmetry group of the bulk bilayer graphene. On the other hand for a short strip $L\ll\ell$, the conductivity becomes isotropic since the change in the momentum upon scattering $(\sim 1/L)$ is much larger than the k-space separation $(1/\ell)$ of the Dirac points and thus their anisotropy will not be revealed anymore.

In conclusion, we have studied conductivity of a wide strip of undoped bilayer graphene which connects two highly doped electrode regions. We have shown that due to the trigonal splitting of Dirac points at zero Fermi energy, the minimal conductivity $\sigma^{\min}$ of the strip finds a dependence on the lattice symmetry axis orientation θ with respect to the electrodes. The anisotropy of $\sigma^{\min}$ depends on the length of strip L as compared to the characteristic length scale $\ell=\pi/\Delta k\simeq 50$ nm determined by the inverse of the k-space separation of two Dirac points. For a short strip of $L\ll\ell$, $\sigma^{\min}$ takes an isotropic universal value $\sigma^{\min}_{\perp}=(8/\pi)e^2/h$. For longer strips the minimal conductivity increases above this value in an anisotropic way. We have found that in the limit of $L\gg\ell$ the anisotropic minimal conductivity grows from $(7/3)\sigma^{\min}_{\perp}$ at $\theta=0$ to $3\sigma^{\min}_{\perp}$ when the orientation is changed by the angle $\Delta\theta\sim\ell/L$.

[1] K. S. Novoselov, A. K. Geim, S. V. Morozov, D. Jiang, Y. Zhang, S. V. Dubonos, I. V. Grigorieva, and A. A. Firsov, Science **306**, 666 (2004).

[2] K. S. Novoselov, A. K. Geim, S. V. Morozov, D. Jiang, M. I. Katsnelson, I. V. Grigorieva, S. V. Dubonos, and A. A. Firsov, Nature (London) **438**, 197 (2005).

[3] Y. Zhang, Y. W. Tan, H. L. Stormer, and P. Kim, Nature (London) **438**, 201 (2005).

[4] K. S. Novoselov, E. McCann, S. V. Morozov, V. I. Fal'ko, M. I. Katsnelson, U. Zeitler, D. Jiang, F. Schedin, and A. K. Geim, Nat. Phys. **2**, 177 (2006).

[5] A. H. Castro Neto, F. Guinea, N. M. R. Peres, K. S. Novoselov, and A. K. Geim, Rev. Mod. Phys. **81**, 109 (2009).

[6] V. V. Cheianov and V. I. Fal'ko, Phys. Rev. B **74**, 041403(R) (2006).

[7] M. I. Katsnelson, K. S. Novoselov, and A. K. Geim, Nat. Phys. **2**, 620 (2006).

[8] E. Fradkin, Phys. Rev. B **33**, 3263 (1986); P. A. Lee, Phys. Rev. Lett. **71**, 1887 (1993).

[9] K. Ziegler, Phys. Rev. Lett. **97**, 266802 (2006).

[10] V. P. Gusynin and S. G. Sharapov, Phys. Rev. Lett. **95**, 146801 (2005); Phys. Rev. B **73**, 245411 (2006).

[11] N. M. R. Peres, F. Guinea, and A. H. Castro Neto, Phys. Rev. B **73**, 125411 (2006).

[12] M. I. Katsnelson, Eur. Phys. J. B **51**, 157 (2006).

[13] P. M. Ostrovsky, I. V. Gornyi, and A. D. Mirlin, Phys. Rev. B **74**, 235443 (2006).

[14] J. Tworzydło, B. Trauzettel, M. Titov, A. Rycerz, and C. W. J. Beenakker, Phys. Rev. Lett. **96**, 246802 (2006).

[15] F. Miao, S. Wijeratne, Y. Zhang, U. C. Coskun, W. Bao, and C. N. Lau, Science **317**, 1530 (2007).

[16] R. Danneau, F. Wu, M. F. Craciun, S. Russo, M. Y. Tomi, J. Salmilehto, A. F. Morpurgo, and P. J. Hakonen, Phys. Rev. Lett. **100**, 196802 (2008).

[17] S. V. Morozov, K. S. Novoselov, M. I. Katsnelson, F. Schedin, D. C. Elias, J. A. Jaszczak, and A. K. Geim, Phys. Rev. Lett. **100**, 016602 (2008).

[18] E. McCann and V. I. Fal'ko, Phys. Rev. Lett. **96**, 086805 (2006).

[19] M. I. Katsnelson, Eur. Phys. J. B **52**, 151 (2006).

[20] J. Cserti, Phys. Rev. B **75**, 033405 (2007).

[21] I. Snyman and C. W. J. Beenakker, Phys. Rev. B **75**, 045322 (2007).

[22] M. Koshino and T. Ando, Phys. Rev. B **73**, 245403 (2006).

[23] J. Cserti, A. Csordás, and G. Dávid, Phys. Rev. Lett. **99**, 066802 (2007).

[24] J. Nilsson, A. H. Castro Neto, F. Guinea, and N. M. R. Peres, Phys. Rev. B **78**, 045405 (2008).

[25] E. V. Castro, K. S. Novoselov, S. V. Morozov, N. M. R. Peres, J. M. B. Lopes dos Santos, J. Nilsson, F. Guinea, A. K. Geim, and A. H. Castro Neto, arXiv:0807.3348 (unpublished).

[26] L. M. Malard, J. Nilsson, D. C. Elias, J. C. Brant, F. Plentz, E. S. Alves, A. H. Castro Neto, and M. A. Pimenta, Phys. Rev. B **76**, 201401(R) (2007).